Inorg. Chem. **2006**, *45*, 4735–4742

Synthesis and Assembly with Mesoporous Silica MCM-48 of Platinum(II) Porphyrin Complexes Bearing Carbazyl Groups: Spectroscopic and Oxygen Sensing Properties

Cheng Huo, Huidong Zhang, Hongyu Zhang, Houyu Zhang, Bing Yang, Ping Zhang,* and Yue Wang*

Key Laboratory for Supramolecular Structure and Materials of Ministry of Education, College of Chemistry, Jilin University, Changchun 130012, People's Republic of China

Received March 2, 2006

The synthesis and spectroscopic characterization of a series of luminescent platinum *meso*-tetrakis{3,5-di[(*N*-carbazyl)*n*-alkyloxyphenyl]}porphyrin (Pt-8C*n*-TPP, *n*-alkyl = $(CH_2)_n$, $n = 4$, 6, and 8) are presented. The protonated platinum porphyrins ([Pt-8C*n*-TPPH8]$^{8+}$) were assembled with mesoporous silica MCM-48 resulting in the assembly materials [Pt-8C*n*-TPPH8]$^{8+}$/MCM-48. The luminescence of [Pt-8C*n*-TPPH8]$^{8+}$/MCM-48 can be extremely quenched by molecular oxygen with very high sensitivity ($I_0/I_{100} > 5000$) and rapid response time (0.04 s) suggesting that the [Pt-8C*n*-TPPH8]$^{8+}$/MCM-48 system can be employed to develop high performance oxygen sensors. Among this assembly system, [Pt-8C8-TPPH8]$^{8+}$/MCM-48 exhibits the highest sensitivity. Even if the concentration of oxygen is 0.1%, the luminescence intensity of [Pt-8C8-TPPH8]$^{8+}$/MCM-48 can be quenched by 86%.

Introduction

Over the past decades, luminescence-based optical oxygen sensors have been largely developed because the determination of molecular oxygen both in the gas and in the liquid phase is very important in many different fields such as analytical chemistry, medical chemistry, and environmental and industrial applications.[1−4] These sensors are based upon the principle that oxygen is a powerful quencher of the luminescent intensity and lifetime of luminescent complexes. The most commonly used complexes for this application are transition metal complexes, especially ruthenium(II) polypyridyl or phenanthroline complexes[5−9] and metalloporphyrins[10−13] owing to their high quantum yields, large Stokes shifts, and long luminescent lifetimes. The host materials used to encapsulate the luminescent complexes are sol−gel and polymer films. Some interesting systems based on sol−gel or polymer immobilized transition metal complexes have been reported.[6,13−16] Over the past decade, it has been demonstrated that mesoporous silicas are excellent host materials for developing functional materials. This is due to the fact that mesoporous silicas have large accessible pore size, high surface areas, and periodic nanoscale pores.[17−36]

* To whom correspondence should be addressed. E-mail: yuewang@jlu.edu.cn. Fax: +86-431-5193421.

(1) Amao, Y.; Miyashita, T.; Okura, I. *Analyst* **2000**, *125*, 871.
(2) Singer, E.; Duveneck, G. L.; Ehrat, M. H.; Widmer, M. *Sens. Actuators, A* **1994**, *42*, 542.
(3) Chan, M. A.; Lam, S. K.; Lo, D. *J. Fluoresc.* **2002**, *12*, 327.
(4) Gao, F. G.; Jeevarajan, A. S.; Anderson, M. M. *Biotechnol. Bioeng.* **2004**, *86*, 425.
(5) Murtagh, M. T.; Shahriari, M. R. *Chem. Mater.* **1998**, *10*, 3862.
(6) Payra, P.; Dutta, P. K. *Microporous Mesoporous Mater.* **2003**, *64*, 109.
(7) Fuller, Z. J.; Bare, W. D.; Kneas, K. A.; Xu, W. Y.; Demas, J. N.; DeGraff, B. A. *Anal. Chem.* **2003**, *75*, 2670.
(8) Yavin, E.; Weiner, L.; Yellin, R. A.; Shanzer, A. *J. Phys. Chem. A* **2004**, *108*, 9274.
(9) García, E. A.; Fernández, R. G.; Díaz-García, M. E. *Microporous Mesoporous Mater.* **2005**, *77*, 235.
(10) Lai, S. W.; Hou, Y. J.; Che, C. M.; Pang, H. L.; Wong, K. Y.; Chang, C. K.; Zhu, N. Y. *Inorg. Chem.* **2004**, *43*, 3724.
(11) Amao, Y.; Asai, K.; Okura, I. *J. Porphyrins Phthalocyanines* **2000**, *4*, 179.
(12) Douglas, P.; Eaton, K. *Sens. Actuators, B* **2002**, *82*, 200.
(13) Gillanders, R. N.; Tedford, M. C.; Crilly, P. J.; Bailey, R. T. *Anal. Chim. Acta* **2004**, *502*, 1.
(14) Lee, S.-K.; Okura, I. *Analyst* **1997**, *122*, 81.
(15) Lee, S.-K.; Okura, I. *Anal. Commun.* **1997**, *34*, 185.
(16) Borisov, S. M.; Vasil'ev, V. V. *J. Anal. Chem.* **2004**, *59*, 155.
(17) Liu, A. M.; Hidajat, K.; Kawi, S.; Zhao, D. Y. *Chem. Commun*. **2000**, 1145.
(18) Luan, Z.; Bae, J. Y.; Kevan, L. *Chem. Mater.* **2000**, *12*, 3202.
(19) Mercier, L.; Pinnavaia, T. J. *Adv. Mater*. **1997**, *9*, 500.
(20) Feng, X.; Fryxell, G. E.; Wang, L. Q.; Kim, A. Y.; Liu, J.; Kemner, K. M. *Science* **1997**, *276*, 923.
(21) Moller, K.; Bein, T. *Chem. Mater.* **1998**, *10*, 2950.
(22) Fowler, C. E.; Lebeau, B.; Mann, S. *Chem. Commun.* **1998**, 1825.
(23) Lim, M. H.; Blanford, C. F.; Stein, A. J. *J. Am. Chem. Soc.* **1997**, *119*, 4090.
(24) Oh, J.; Imai, H.; Hirashima, H. *Chem. Mater.* **1998**, *10*, 1582.
(25) Honma, I.; Zhou, H. S. *Adv. Mater.* **1998**, *10*, 1532.
(26) Wu, C. G.; Bein, T. *Science* **1994**, *264*, 1757.

10.1021/ic060354c CCC: $33.50
Published on Web 05/11/2006

Previous reports have demonstrated that high sensitivity or fast response could be achieved, respectively, for some transition metal complex based oxygen sensors.[37−41] However, few of these oxygen sensors simultaneously displayed high sensitivity and fast response. The design and assembly of high performance oxygen sensors based on luminescent transition metal complexes remain a challenge for chemists. To obtain more efficient oxygen sensing materials, the design and synthesis of new luminescent complexes and optimization of assembly systems should be the focus. In this contribution, we report the synthesis of a series of alkyl−carbazole substitute platinum porphyrin complexes (Pt-8C*n*-TPP) and the assembly of [Pt-8C*n*-TPPH8]$^{8+}$ with mesoporous silica MCM-48. The optical oxygen sensing properties of assembly materials [Pt-8C*n*-TPPH8]$^{8+}$/MCM-48 also will be presented.

Experimental Section

Materials. Pyrrole, boron tribromide, 1,4-dibromobutane, 1,6-dibromohexane, 1,8-dibromooctane, and platium(II) chloride were purchased form Aldrich. 3,5-Dimethoxybenzaldehyde and carbazole were obtained from Acros. All the other chemicals were obtained from Tianjin Tiantai Pure Chemicals Co., Ltd. Tetrakis(3,5-dihydroxyphenyl)porphyrin (see Supporting Information)[42] and *N*-(8-bromooctyl)carbazole[43] were synthesized according to the literature procedures. Mesoporous silica (MCM-48) was hydrothermally prepared following literature procedures.[44] Then the template was removed from the mesoporous silicate by calcinations at 560 °C for 8 h.

***meso*-Tetrakis{3,5-di[(*N*-carbazyl)*n*-octyloxyphenyl]}porphyrin (8C8-TPP).** Under nitrogen, tetrakis(3,5-dihydroxyphenyl)-porphyrin (0.74 g, 1 mmol) was added to 500 mL of *N*′,*N*′-dimethyl formamide (DMF) with K_2CO_3 (1.4 g, 10 mmol). The mixture was heated to reflux for 1 h, and then *N*-(8-bromooctyl)carbazole (4.3 g, 12 mmol) was added. Heating the mixture to reflux for 10 h was continued. After distilling off DMF, the residue was purified by column chromatography using silica gel with dichloromethane as eluent (yield 35%). ^{1}H NMR (500 MHz, $CDCl_3$, 25 °C, TMS): δ = 8.90 (s, 8H), 8.05 (d, J = 2.0 Hz, 16H), 7.41 (t, J = 8.5 Hz, 16H), 7.33 (s, 8H), 7.27 (m, 32H), 6.80 (t, J = 2.0 Hz, 4H), 4.32 (t, J = 7.0 Hz, 16H), 4.06 (t, J = 6.0 Hz, 16H), 2.07 (m, 16H), 1.89 (m, 16H), 1.38 (m, 64H), −2.84 (s, 2H). MS *m*/*z* (%): 2962.1 (100) [M$^+$]. Elem anal. Calcd (%) for $C_{204}H_{214}N_{12}O_8$: C, 82.72; H, 7.28; N, 5.67. Found: C, 82.63; H, 7.46; N, 5.51.

***meso*-Tetrakis{3,5-di[(*N*-carbazyl)*n*-hexyloxyphenyl]}porphyrin (8C6-TPP).** The title compound was prepared by the same procedure as *meso*-tetrakis{3,5-di[(*N*-carbazyl)*n*-octyloxyphenyl]}-porphyrin (yield 32%). ^{1}H NMR (500 MHz, $CDCl_3$, 25 °C, TMS): δ = 8.91 (s, 8H), 7.99 (d, J = 7.5 Hz, 16H), 7.34 (m, 40H), 7.11 (t, J = 6.5 Hz, 16H), 6.81 (t, J = 2.0 Hz, 4H), 4.25 (t, J = 7.5 Hz, 16H), 4.02 (t, J = 6.5 Hz, 16H), 1.86 (m, 16H), 1.77 (m, 16H), 1.49 (m, 16H), 1.42 (m, 16H), −2.80 (s, 2H). MS *m*/*z* (%): 2737.7 (100) [M$^+$]. Elem anal. Calcd (%) for $C_{188}H_{182}N_{12}O_8$: C, 82.48; H, 6.70; N, 6.14. Found: C, 82.40; H, 6.85; N, 6.09.

***meso*-Metrakis{3,5-di[(*N*-carbazyl)*n*-butyloxyphenyl]}porphyrin (8C4-TPP).** The title compound was prepared by the same procedure as *meso*-tetrakis{3,5-di[(*N*-carbazyl)*n*-octyloxyphenyl]}-porphyrin (yield 37%). ^{1}H NMR (500 MHz, $CDCl_3$, 25 °C, TMS): δ = 8.86 (s, 8H), 8.03 (d, J = 7.5 Hz, 16H), 7.38 (m, 32H), 7.30 (d, J = 2.0 Hz, 8H), 7.15 (t, J = 7.0 Hz, 16H), 6.78 (t, J = 2.0 Hz, 4H), 4.38 (t, J = 7.0 Hz, 16H), 4.05 (t, J = 6.0 Hz, 16H), 2.10 (m, 16H), 1.90 (m, 16H), −2.88 (s, 2H). MS *m*/*z* (%): 2513.4 (100) [M$^+$]. Elem anal. Calcd (%) for $C_{172}H_{150}N_{12}O_8$: C, 82.20; H, 6.02; N, 6.69. Found: C, 82.08; H, 6.13; N, 6.54.

Platinum *meso*-Tetrakis{3,5-di[(*N*-carbazyl)*n*-octyloxyphenyl]}porphyrin (Pt-8C8-TPP). Under nitrogen, $PtCl_2$ (50 mg, 0.2 mmol) and 8C8-TPP (60 mg, 0.02 mmol) were suspended in 100 mL of benzonitrile. The mixture was then heated to reflux for 10 h. The mixture was cooled to room temperature, and the solvent was removed by vacuum distillation. The crude product was purified by column chromatography using silica gel with dichloromethane as the eluent (yield 99%). ^{1}H NMR (500 MHz, $CDCl_3$, 25 °C, TMS): δ = 8.84 (s, 8H), 8.02 (d, J = 7.5 Hz, 16H), 7.36 (t, J = 7.5 Hz, 16H), 7.31 (d, J = 8.5 Hz, 16H), 7.27 (d, J = 2.0 Hz, 8H), 7.13 (t, J = 7.5 Hz, 16H), 6.82 (t, J = 2.0 Hz, 4H), 4.20 (t, J = 7.0 Hz, 16H), 4.02 (t, J = 6.5 Hz, 16H), 1.78 (m, 32H), 1.49 (m, 16H), 1.41 (m, 16H), 1.30 (m, 32H). MS *m*/*z* (%): 3155.8 (100) [M$^+$]. Elem anal. Calcd (%) for $C_{204}H_{212}N_{12}O_8Pt$: C, 77.66; H, 6.77; N, 5.33. Found: C, 77.53; H, 6.91; N, 5.28.

Platinum *meso*-Tetrakis{3,5-di[(*N*-carbazyl)*n*-hexyloxyphenyl]}porphyrin (Pt-8C6-TPP). The title compound was prepared by the same procedure as Pt-8C8-TPP (yield 98%). ^{1}H NMR (500 MHz, $CDCl_3$, 25 °C, TMS): δ = 8.82 (s, 8H), 7.95 (d, J = 7.5 Hz, 16H), 7.33 (m, 32H), 7.23 (d, J = 2.0 Hz, 8H), 7.08 (t, J = 7.5 Hz, 16H), 6.79 (t, J = 2.0 Hz, 4H), 4.24 (t, J = 7.0 Hz, 16H), 4.00 (t, J = 6.5 Hz, 16H), 1.86 (m, 16H), 1.77 (m, 16H), 1.49 (m, 16H), 1.41 (m, 16H). MS *m*/*z* (%): 2931.2 (100) [M$^+$]. Elem anal. Calcd (%) for $C_{188}H_{180}N_{12}O_8Pt$: C, 77.05; H, 6.19; N, 5.74. Found: C, 77.01; H, 6.38; N, 5.62.

Platinum *meso*-Tetrakis{3,5-di[(*N*-carbazyl)*n*-butyloxyphenyl]}porphyrin (Pt-8C4-TPP). The title compound was prepared by the same procedure as Pt-8C8-TPP (yield 98%). ^{1}H NMR (500 MHz, $CDCl_3$, 25 °C, TMS): δ = 8.76 (s, 8H), 8.01 (d, J = 8.0 Hz, 16H), 7.37 (m, 32H), 7.23 (d, J = 2.5 Hz, 8H), 7.14 (t, J = 7.0 Hz, 16H), 6.76 (t, J = 2.0 Hz, 4H), 4.38 (t, J =

(27) Xiang, S.; Zhang, Y. L.; Xin, Q.; Li, C. *Angew. Chem., Int. Ed.* **2002**, *41*, 821.
(28) Han, H. B.; Manners, I.; Winnik, M. A. *Chem. Mater.* **2005**, *17*, 3160.
(29) Zhang, H. D.; Sun, Y. H.; Ye, K. Q.; Zhang, P.; Wang, Y. *J. Mater. Chem.* **2005**, *15*, 3181.
(30) Liu, X. Y.; Tian, B. Z.; Yu, C. Z.; Gao, F.; Xie, S. H.; Tu, B.; Che, R. C.; Peng, L. M.; Zhao, D. Y. *Angew. Chem., Int. Ed.* **2002**, *41*, 3876.
(31) Shen, S. D.; Garcia-Bennett, A. E.; Liu, Z.; Liu, Q. Y.; Shi, Y. F.; Yan, Y.; Yu, C. Z.; Liu, W. C.; Cai, Y.; Terassaki, O.; Zhao, D. Y. *J. Am. Chem. Soc.* **2005**, *127*, 6780.
(32) Wirnsberger, G.; Scott, B. J.; Stucky, G. D. *Chem. Commun.* **2001**, 119.
(33) Scott, B. J.; Wirnsberger, G.; Stucky, G. D. *Chem. Mater.* **2001**, *13*, 3140.
(34) Corma, A.; Galletero, M. S.; Garcia, H.; Palomares, E.; Rey, F. *Chem. Commun.* **2002**, 1100.
(35) Furukawa, H.; Watanabe, T.; Kuroda, K. *Chem. Commun.* **2001**, 2002.
(36) Alvaro, M.; Ferrer, B.; Garcia, H.; Rey, F. *Chem. Commun.* **2002**, 2012.
(37) Amao, Y.; Asai, K.; Miyashita, T.; Okura, I. *Polym. Adv. Technol.* **2000**, *11*, 705.
(38) Amao, Y.; Miyashita, T.; Okura, I. *J. Porphyrins Phthalocyanines* **2001**, *5*, 433.
(39) Klimant, I.; Wolfbeis, O. S. *Anal. Chem.* **1995**, *67*, 3160.
(40) Mills, A.; Thomas, M. *Analyst* **1997**, *122*, 63.
(41) Mills, A.; Lepre, A. *Anal. Chem.* **1997**, *69*, 4653.
(42) Zimmerman, S. C.; Zharov, I.; Wendland, M. S.; Rakow, N. A.; Suslick, K. S. *J. Am. Chem. Soc.* **2003**, *125*, 13504.
(43) Manickam, M.; Belloni, M.; Kumar, S.; Varshney, S. K.; Rao, D. S. S.; Ashton, P. R.; Preece, J. A.; Spencer, N. *J. Mater. Chem.* **2001**, *11*, 2790.
(44) Beck, J. S.; Vartuli, J. C.; Roth, W. J.; Leonowicz, E. M.; Kresge, C. T.; Schmitt, K. D.; Chu, C. T.-W.; Olson, D. H.; Sheppard, E. W.; McCullen, S. B.; Higgins, J. B.; Schlenker, J. L. *J. Am. Chem. Soc.* **1992**, *114*, 10834.

7.0 Hz, 16H), 4.03 (t, J = 6.0 Hz, 16H), 2.09 (m, 16H), 1.87 (m, 16H). MS m/z (%): 2706.9 (100) [M^+]. Elem anal. Calcd (%) for $C_{172}H_{148}N_{12}O_8Pt$: C, 76.34; H, 5.51; N, 6.21. Found: C, 76.17; H, 5.64; N, 6.29.

[Pt-8C*n*-TPPH8]$^{8+}$/MCM-48. The platinum porphyrins were immobilized into MCM-48 by the following procedure. For example, 1 mg of Pt-8C8-TPP and 0.2 mL (10^{-2} M) of trifluoroacetic acid tetrahydrofuran (THF) solution were added into 10 mL of a THF/water (v/v = 0.65:0.35) mixture solution, and the mixture was stirred for 5 min. Titration experiments demonstrated that there are eight protons per Pt-8C8-TPP molecule under these conditions. Then 50 mg of MCM-48 was added, and stirring of the mixture solution was continued for 1 h at room temperature. The resulting [Pt-8C8-TPPH8]$^{8+}$/MCM-48 solid powders were filtered off to give an orange powder product. The orange powders were washed repeatedly with THF/water solution three times. UV−vis spectroscopy investigation revealed that no platinum porphyrin existed in the filtered washing solution, suggesting that all of platinum porphyrin molecules were immobilized onto the MCM-48 surface. The residual powders were dried in air to obtain the target sample, [Pt-8C8-TPPH8]$^{8+}$/MCM-48 (20 mg/g). The samples with different [Pt-8C8-TPPh8]$^{8+}$ loading levels (10, 20, and 40 mg [Pt-8C8-TPPH8]$^{8+}$/g MCM-48) were prepared by altering the concentrations of initial solution of Pt-8C8-TPP. UV−vis monitoring results showed that if the weight of the platinum porphyrin sample was not more than 4 mg and that of MCM-48 was 50 mg, no platinum porphyrin molecules existed in the residue solution. Other platinum porphyrin complexes were incorporated into MCM-48 with procedure similar to that described above.

Photoluminescence and Quantum Yields Measurements. Fluid solution emission samples were freeze−pump−thaw cycled with a high vacuum. The room-temperature luminescence quantum yields were referenced to platinum *meso*-tetrakis(phenyl)porphyrin (PtTPP, Φ = 0.046)[45] and calculated according to the following equation:

$$\Phi_{unk} = \Phi_{std}(I_{unk}/A_{unk})(A_{std}/I_{std})(\eta_{unk}/\eta_{std})^2$$

where Φ_{unk} is the radiative quantum yield of the sample, Φ_{std} is the radiative quantum yield of the standard, I_{unk} and I_{std} are the integrated emission intensities of the sample and standard, respectively, A_{unk} and A_{std} are the absorptions of the sample and standard at the excitation wavelength, respectively, and η_{unk} and η_{std} are the indexes of refraction of the sample and standard solutions (pure solvents were assumed), respectively.

Oxygen Sensing Properties Measurement. Each platinum porphyrin/MCM-48 sample was fixed inside a laboratory-made cell that was equipped with two quartz windows and an airtight stopper which had inlet and outlet lines to allow gas flow. To investigate the sensing properties of samples under different oxygen concentrations, dry nitrogen and dry oxygen were mixed to obtain gas mixtures containing well-defined oxygen concentrations using two gas flowers to control the relative flow rates of nitrogen and oxygen, respectively. All experiments were carried out in the dark at room temperature. The emission spectra and response curves were recorded with a PTI emission spectrophotometer.

Molecular Modeling of the Conformation. The molecular modeling of a series of protonated platinum porphyrin complexes was performed with combined quantum-mechanical and molecular mechanics methods. The software package used for the molecular modeling studies was the Cerius 2 software package. We modeled different parts of the system with different techniques. For the rigid planar platinum *meso*-tetrakis-phenyl porphyrin core, an ab initio geometry optimized calculation was used for the model. The complete system then was modeled using molecular mechanics, by holding the geometry of the platinum porphyrin center region fixed and optimizing the rest of the molecule.

Scheme 1. Synthesis Procedure of Platinum Porphyrins Pt-8C*n*-TPP and Their Protonated Complexes [Pt-8C*n*-TPPH8]$^{8+}$ and the Molecular Structure of [PtTMPy]$^{4+}$

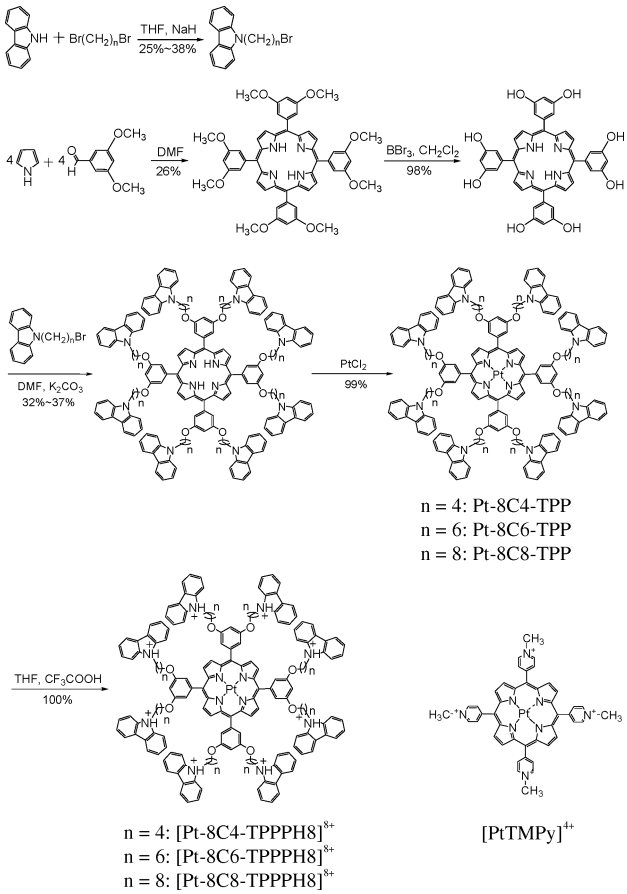

Characterization. The powder X-ray diffraction (XRD) patterns were recorded on a Siemens D5005 diffractometer with Cu Kα radiation. ^{1}H NMR spectra were recorded on Bruker Avance 500 MHz spectrometer with tetramethylsilane as the internal standard. Mass spectra were recorded on a GC/MS mass spectrometer. Absorption spectra were obtained using a PE UV−vis Lambda 20 spectrometer. Photoluminescence spectra were collected by a PTI emission spectrophotometer. Nitrogen adsorption−desorption experiments were performance on an Autosorb-1 at 77 K.

Results and Discussion

Preparation and Spectroscopic Characterization. The synthetic procedures of platinum(II) carbazole substituted porphyrin complexes used in this study are shown in Scheme 1, which generally affords superior yields. Figure 1 shows the absorption and emission spectra of Pt-8C8-TPP in dichloromethane solution (oxygen free). The absorption bands, which are located in the UV region, are mainly attributed to carbazole units, and the intense Soret band appears at 404 nm with the weaker Q bands appearing at 510 and 540 nm. Pt-8C8-TPP displays a typical platinum(II) porphyrin emission feature, and the emission maximum appears at 654 nm. The absorption and emission spectra of

(45) Che, C. M.; Hou, Y. J.; Chan, M. C. W.; Guo, J.; Liu, Y.; Wang, Y. *J. Mater. Chem.* **2003**, *13*, 1362.

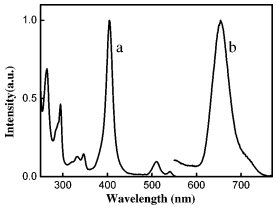

Figure 1. Absorption (a) and emission (b) spectra of Pt-8C8-TPP in degassed dichloromethane solution at 298 K.

Table 1. Emission Data and the Photoluminescent Quantum Yields of Pt-8C4-TPP and [Pt-8C*n*-TPPH8]$^{8+}$ in Solution at 298 K

complex	λ_{max}, nm	Φ_F[a]
Pt-8C4-TPP	655	0.11
Pt-8C6-TPP	655	0.09
Pt-8C8-TPP	654	0.10
[Pt-8C4-TPPH8]$^{8+}$	660	0.10
[Pt-8C6-TPPH8]$^{8+}$	659	0.09
[Pt-8C8-TPPH8]$^{8+}$	658	0.11

[a] Φ_F values were referenced to PtTPP ($\Phi_F = 0.046$), ref 45.

Pt-8C4-TPP and Pt-8C6-TPP in solution show a similar profile with that of Pt-8C8-TPP, regardless of the alkyl spacer chain length (see Supporting Information, Figures S1-S2). The photoluminescent quantum yields (Φ_F) of Pt-8C*n*-TPP are presented in Table 1. At room temperature, Pt-8C4-TPP, Pt-8C6-TPP, and Pt-8C8-TPP display relatively higher photoluminescence quantum yields in solution compared with PtTPP.[45] Under air atmosphere, the emission intensities of Pt-8C*n*-TPP solutions are much weaker compared with that recorded for oxygen free solutions (see Supporting Information, Figures S3−S5). Although we cannot quantitatively measure the oxygen concentration-dependent emission spectra of Pt-8C*n*-TPP in solution because of the limitations of our equipment, the experiment results suggest that oxygen molecules could efficiently quench the emission of Pt-8C*n*-TPP in solution. The oxygen concentration-dependent emission spectra of the solid powders of Pt-8C*n*-TPP show that oxygen molecules could lead to the emission quenching of Pt-8C*n*-TPP, but quenching degrees are relatively low (see Supporting Information, Figures S6−S8).

Treating Pt-8C*n*-TPP with trifluoroacetic acid resulted in protonated porphyrins [Pt-8C*n*-TPPH8]$^{8+}$, which were employed as chromophores to assemble oxygen sensors with mesoporous silica MCM-48. It was found that the neutral platinum porphyrins (Pt-8C*n*-TPP) could not be immobilized into MCM-48. In contrast, the protonated porphyrins [Pt-8C*n*-TPPH8]$^{8+}$ can be easily immobilized into MCM-48. This may be attributed to the fact that carbazole ions could be adsorbed into the pores of MCM-48 by the interaction of cation exchange with the protons of silanol groups on the surface of MCM-48.[28,29,46,47] Although the detailed adsorption process has not been determined, the protonation of carbazole groups is crucial for the immobilization of the platinum porphyrin molecules into MCM-48. It is worth noting that [Pt-8C*n*-TPPH8]$^{8+}$ complexes cannot be adsorbed by the templated filled MCM-48 and only the calcinated MCM-48 can be used to prepare assembly materials [Pt-8C*n*-TPPH8]$^{8+}$/MCM- 48.

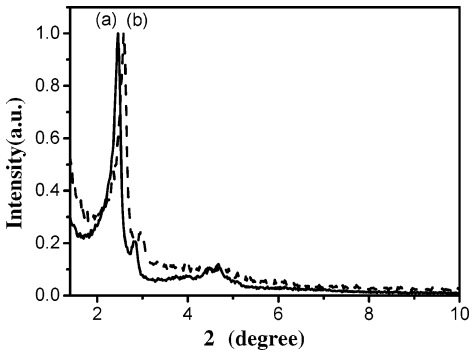

Figure 2. Powder X-ray spectra of MCM-48 (a) and [Pt-8C8-TPPH8]$^{8+}$/MCM-48 (20 mg/g; b).

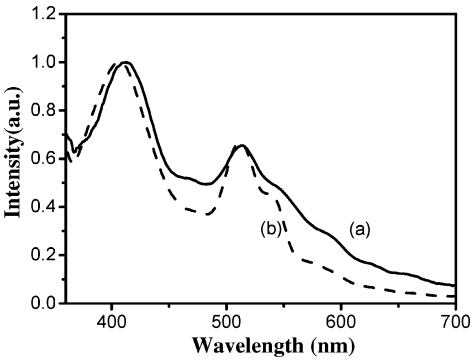

Figure 3. UV−visible diffuse spectra of [Pt-8C8-TPPH8]$^{8+}$ in the solid state (a) and [Pt-8C8-TPPH8]$^{8+}$/MCM-48 (20 mg/g; b).

The XRD patterns (Figure 2) of [Pt-8C8-TPPH8]$^{8+}$/MCM-48 (20 mg/g) show similar patterns, and the high-intensity Bragg peak shifted slightly to a higher angle compared with that of MCM-48. It indicates that, after adsorption of [Pt-8C8-TPPH8]$^{8+}$, the cubic arrangement of channels in [Pt-8C8-TPPH8]$^{8+}$/MCM-48 remains unchanged and the cell parameter *a* decreases slightly. The UV−vis diffuse spectrum of [Pt-8C8-TPPH8]$^{8+}$/MCM-48 (20 mg/g) shows a profile similar to that of [Pt-8C8-TPPH8]$^{8+}$ in the solid state (Figure 3) suggests that [Pt-8C8-TPPH8]$^{8+}$ molecules are immobilized into MCM-48. The nitrogen adsorption−desorption isotherms measured at 77 K for the calcined MCM-48 and [Pt-8C8-TPPH8]$^{8+}$/MCM-48 are shown in Figure 4, which display typical IV curves. The Brunauer−Emmett−Teller (BET) surface areas are 1332 m^2/g and 1085 m^2/g, for calcined MCM-48 and [Pt-8C8-TPPH8]$^{8+}$/MCM-48, respectively. The calcined MCM-48 exhibits a narrow pore size distribution with a mean value of 2.7 nm. [Pt-8C8-TPPH8]$^{8+}$/MCM-48 also displays a narrow pore size distribution with a mean value of 2.2 nm. The relatively small pore diameter and surface area of [Pt-8C8-TPPH8]$^{8+}$/MCM-48 should be attributed to the organic groups that remain in the pores. It is also possible that the incorporation of organic groups leads to slight rearrangement of the pores. The nitrogen absorption−desorption results also show that the ordered cubic arrangement of pores of MCM-48 remains unchanged after Pt−porphyrin molecules are incorporated,

(46) Fang, M.; Wang, Y.; Zhang, P.; Li, S. G.; Xu, R. R. *J. Luminesc.* **2000**, *91*, 67.
(47) Zhang, P.; Guo, J. H.; Wang, Y.; Pang, W. Q. *Mater. Lett.* **2002**, *53*, 400.

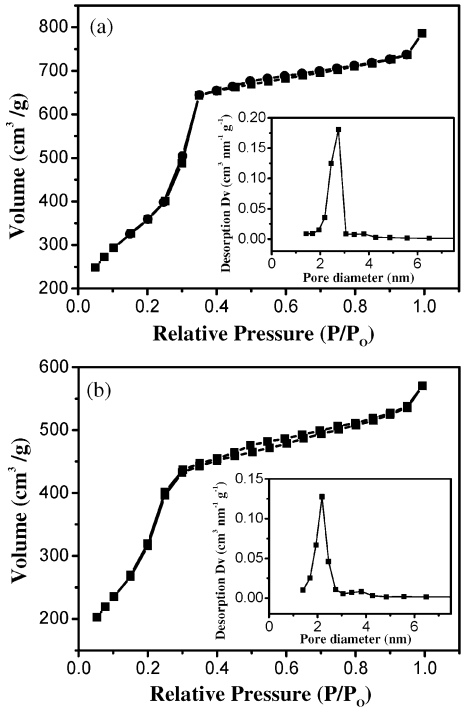

Figure 4. Nitrogen adsorption−desorption isotherm (77 K) of the calcined MCM-48 (a) and [Pt-8C8-TPPH8]$^{8+}$/MCM-48 (b). Insets: Corresponding pore distributions.

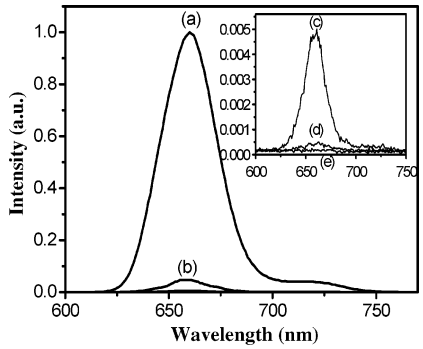

Figure 5. Emission spectra of [Pt-8C8-TPPH8]$^{8+}$/MCM-48 (20 mg/g) under different oxygen concentrations: (a) 0; (b) 0.1; (c) 1; (d) 10, and (e) 100% oxygen.

although slight decrease of the pore diameter of MCM-48 takes place.

Oxygen Sensing Properties. The luminescence of platinum porphyrin complexes could be quenched efficiently by molecular oxygen. The mechanism of the quenching process consists of the exchange energy transfer from the lowest triplet excited state of metalloporphyrin to molecular oxygen, which is accompanied by the formation of singlet oxygen. As a result, these complexes could be commonly used to develop oxygen-sensing materials. The oxygen concentration-dependent emission spectra of [Pt-8C8-TPPH8]$^{8+}$/MCM-48 (20 mg/g) are shown in Figure 5. The emission maximum of [Pt-8C8-TPPH8]$^{8+}$/MCM-48 (20 mg/g) is at 660 nm and is constant under different oxygen concentrations. However, the relative intensity decreased markedly upon increasing oxygen concentration. The variations of the emission spectra of [Pt-8C8-TPPH8]$^{8+}$/MCM-48 (10 or 40 mg/g) display similar trends to that of [Pt-8C8-TPPH8]$^{8+}$/MCM-48 (20 mg/g). The relative luminescent intensities of [Pt-8C8-TPPH8]$^{8+}$/MCM-48 (10 mg/g), [Pt-8C8-TPPH8]$^{8+}$/MCM-48 (20 mg/g), and [Pt-8C8-TPPH8]$^{8+}$/MCM-48 (40 mg/g) decrease by 99.93, 99.98%, and 99.97%, respectively, upon changing from pure nitrogen to pure oxygen conditions. [Pt-8C8-TPPH8]$^{8+}$/MCM-48 (20 mg/g) is more sensitive compared with [Pt-8C8-TPPH8]$^{8+}$/MCM-48 (10 mg/g) and [Pt-8C8-TPPH8]$^{8+}$/MCM-48 (40 mg/g), suggesting that the optimum loading level is 20 mg/g. Under 100% nitrogen, [Pt-8C8-TPPH8]$^{8+}$/MCM-48 (20 mg/g) shows a stronger emission intensity compared with [Pt-8C8-TPPH8]$^{8+}$/MCM-48 (10 mg/g) and [Pt-8C8-TPPH8]$^{8+}$/MCM-48 (40 mg/g; see Supporting Information, Figure S35). These results provide a possible explanation for the optimum loading level.

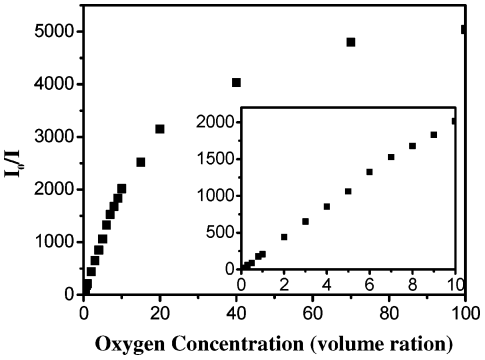

Figure 6. Stern−Volmer plot for [Pt-8C8-TPPH8]$^{8+}$/MCM-48 (20 mg/g) at different concentrations of oxygen. (I_0 and I are luminescent intensities in the absence and in the presence of oxygen.) Inset: Stern−Volmer plot at low oxygen concentration.

The Stern−Volmer plot for [Pt-8C8-TPPH8]$^{8+}$/MCM-48 (20 mg/g) is shown in Figure 6. The I_0/I_{100} ratio (I_0 and I_{100} are the luminescent intensities in the absence and in the presence of oxygen, respectively) has been used as an indicator of the sensitivity of the sensing device, and a sensor with I_0/I_{100} more than 3.0 is a suitable oxygen sensing device.[48] The value of I_0/I_{100} of [Pt-8C8-TPPH8]$^{8+}$/MCM-48 (20 mg/g) is 5041.2. To our knowledge, it is the highest value for optical oxygen sensors based on platinum porphyrins that has been achieved until now. The optical oxygen sensor reported previously displayed a maximum I_0/I_{100} of 682.5.[49] The plot is nonlinear within a wide range of oxygen concentrations. It has been demonstrated that, for the heterogeneous system, Stern−Volmer plots for the sensor systems based on luminescence quenching often display a nonlinear feature within a wide range of oxygen concentrations,[50−52] which is attributed to the simultaneous presence of static and dynamic quenching and the inequality of the microenvironment of the immobilized lumophore molecules in the matrix.[53,54] Close investigation reveals that the Stern−Volmer

(48) MacCraith, B. D.; McDonagh, C. M.; O'Keeffe, G.; Keyes, E. T.; Vos, J. G.; O'Kelly, B.; McGilp, J. F. *Analyst* **1993**, *118*, 385.
(49) Amao, Y.; Miyashita, T.; Okura, I. *J. Porphyrins Phthalocyanines* **2001**, *5*, 433.
(50) Xu, W.; Schmidt, R.; Whaley, M.; Demas, J. N.; DeGraff, B. A.; Karikari, E. K.; Farmer, B. L. *Anal. Chem.* **1995**, *67*, 3172.
(51) Carraway, E. R.; Demas, J. N.; DeGraff, B. A.; Bacon, J. R. *Anal. Chem.* **1991**, *63*, 337.
(52) Lakowicz, J. R. *Principle of Fluorescence Spectroscopy*; Plenum: New York, 1986; p 266.

Table 2. Oxygen Sensing Properties of Different Platinum Porphyrin Complexes Incorporated in MCM-48

	[Pt-8C8-TPPH8]$^{8+}$/MCM-48			[Pt-8C6-TPPH8]$^{8+}$/MCM-48			[Pt-8C4-TPPH8]$^{8+}$/MCM-48			[PtTMPyP]$^{4+}$/MCM-48		
	10 mg/g	20 mg/g	40 mg/g	10 mg/g	20 mg/g	40 mg/g	10 mg/g	20 mg/g	40 mg/g	10 mg/g	20 mg/g	40 mg/g
$I_0/I_{0.1}$	6.5	21.5	20.8	6.0	7.1	6.8						
I_0/I_1	60.6	208.1	209.2	44.9	65.1	64.0				3.2	3.7	2.5
I_0/I_{10}	552.8	2016.3	1728.5	437.8	604.4	493.3	1.5	1.5	1.4	13.4	20.5	9.5
I_0/I_{100}	1488.6	5041.2	3961.5	1302.6	2015.2	1627.5	5.3	5.7	4.1	23.6	49.6	20.9
$t\downarrow$ (95%), s	0.06	0.04	0.04	0.04	0.06	0.06	1.00	1.20	1.40	0.40	0.40	0.40
$t\uparrow$ (95%), s	24.80	32.20	55.50	40.50	28.30	50.80	7.02	7.20	8.60	15.80	14.40	11.04

plot exhibits considerable linearity when the concentration of oxygen varies from 0 to 10% (inset of Figure 6). The plot indicates that high sensitivity is achieved in the oxygen concentration range of 0−10%. Even when the concentration of oxygen is only 0.1%, the quenching of [Pt-8C8-TPPH8]$^{8+}$/MCM-48 (20 mg/g) can reach 95.35% ($I_0/I_{0.1} = 21.5$, $I_{0.1}$ is the luminescent intensity in the presence of oxygen with 0.1% concentration.). It is well-known that the measurement of oxygen at low concentration is more important, so [Pt-8C8-TPPH8]$^{8+}$/MCM-48 has a great potential for application in oxygen sensors.

For oxygen sensors the response time is also very important. Generally, a 95% response time, that is, $t\downarrow$ (95%, N_2 to O_2), is defined as the time required for luminescent intensity to decrease by 95% on changing from 100% nitrogen to 100% oxygen. Similarly, 95% recovery time, that is, $t\uparrow$ (95%, O_2 to N_2), means the time required for luminescent intensity to reach the 95% of the initial value recorded under 100% nitrogen on changing from 100% oxygen to 100% nitrogen. Figure 7 shows the response property of [Pt-8C8-TPPH8]$^{8+}$/MCM-48 (20 mg/g). Upon increasing oxygen concentration, the emission intensity drops very quickly, while upon decreasing oxygen concentration, the emission intensity increases and recovers to the initial level under 100% nitrogen again. This cycle is repeated; the emission intensity changes are monitored when the sample is exposed to an alternating atmosphere of nitrogen and oxygen, and it is observed that the emission intensity changes are reversible. The response time $t\downarrow$ (95%, N_2 to O_2) and recovery time $t\uparrow$ (95%, O_2 to N_2) of [Pt-8C8-TPPH8]$^{8+}$/MCM-48 (20 mg/g) are 0.04 and 32.20 s, respectively. To our knowledge, it is the fastest response time for oxygen sensors based on metal porphyrins. The optical oxygen sensor reported previously displayed the fastest response of 0.33 s.[29] The recovery time of [Pt-8C8-TPPH8]$^{8+}$/MCM-48 (20 mg/g) is not short enough compared with its response time. A possible explanation is that the sensitivity of [Pt-8C8-TPPH8]$^{8+}$/MCM-48 (20 mg/g) is extremely high, and a trace of oxygen can efficiently quench its luminescence. Because of the limitation of the laboratory-made cell that we used, a certain time has to be spent to change the system from oxygen to nitrogen completely. Minimizing the recovery time should be possible if the oxygen can depart from the sensor more quickly by modifying the cell. Another explanation is that for [Pt-8C8-TPPH8]$^{8+}$/MCM-48 the oxygen desorption rate is not very fast.

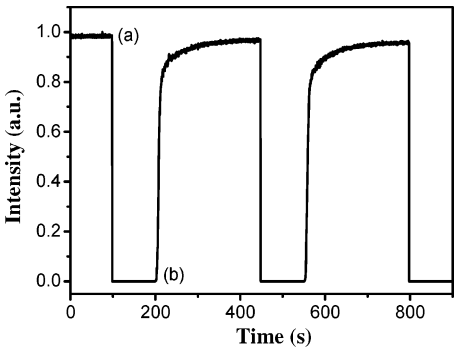

Figure 7. Response time and relative intensity change and reproducibility for [Pt-8C8-TPPH8]$^{8+}$/MCM-48 (20 mg/g) on switching between 100% nitrogen (a) and 100% oxygen (b).

Performance Comparison. To optimize platinum porphyrin/MCM-48 sensing materials, a series of alkyl−carbazole substituted platinum porphyrins with different lengths of alkyl chains (Scheme 1) were synthesized and employed to assemble sensors with MCM-48. The oxygen sensing properties of [Pt-8C*n*-TPPH8]$^{8+}$/MCM-48 are summarized in Table 2 (the detailed spectra are collected in Supporting Information, Figures S9−S34). By comparison we can conclude that the [Pt-8C8-TPPH8]$^{8+}$/MCM-48 system exhibits the best oxygen sensing performance. For the [Pt-8C*n*-TPPH8]$^{8+}$/MCM-48 ($n = 8, 6, 4$) series, the oxygen sensing performance clearly shows an upward tendency with increasing the lengths of alkyl chains. The oxygen sensing properties of [Pt-8C8-TPPH8]$^{8+}$/MCM-48 and [Pt-8C6-TPPH8]$^{8+}$/MCM-48 are similar to each other, while that of [Pt-8C4-TPPH8]$^{8+}$/MCM-48 is not very outstanding. Nitrogen adsorption−desorption study shows that the MCM-48 sample used in this study has a narrow pore size distribution with a mean value of 2.7 nm. Molecular simulation calculation results revealed that [Pt-8C8-TPPH8]$^{8+}$, [Pt-8C6-TPPH8]$^{8+}$, and [Pt-8C4-TPPH8]$^{8+}$ have approximate dimensions of 2.6 nm × 2.6 nm × 3.1 nm, 2.6 nm × 2.6 nm × 2.5 nm, and 1.9 nm × 1.9 nm × 2.0 nm, respectively (Figure 8). Therefore, [Pt-8C8-TPPH8]$^{8+}$ or [Pt-8C6-TPPH8]$^{8+}$ molecules with bigger size cannot be wholly adsorbed into the pores of MCM-48 and can only be immobilized onto the exo-surface of MCM-48 by inserting their alkyl−carbazole arms into the pores of MCM-48 and lifting the porphyrin cores outside. This assembly form enhances the effective collisions between the chromophores and the oxygen molecules resulting in the fact that the phosphorescences of [Pt-8C8-TPPH8]$^{8+}$/MCM-48 and [Pt-8C6-TPPH8]$^{8+}$/MCM-48 are very sensitive to oxygen. In contrast, the [Pt-8C4-TPPH8]$^{8+}$ molecules can be wholly adsorbed into the pore of MCM-48, because that the pore diameter of

(53) Hartmann, P.; Leiner, M. J. P.; Lippitsch, M. E. *Anal. Chem.* **1995**, *67*, 88.
(54) Lippitsch, M. E.; Draxler, S. *Sens. Actuators, B* **1993**, *11*, 97.

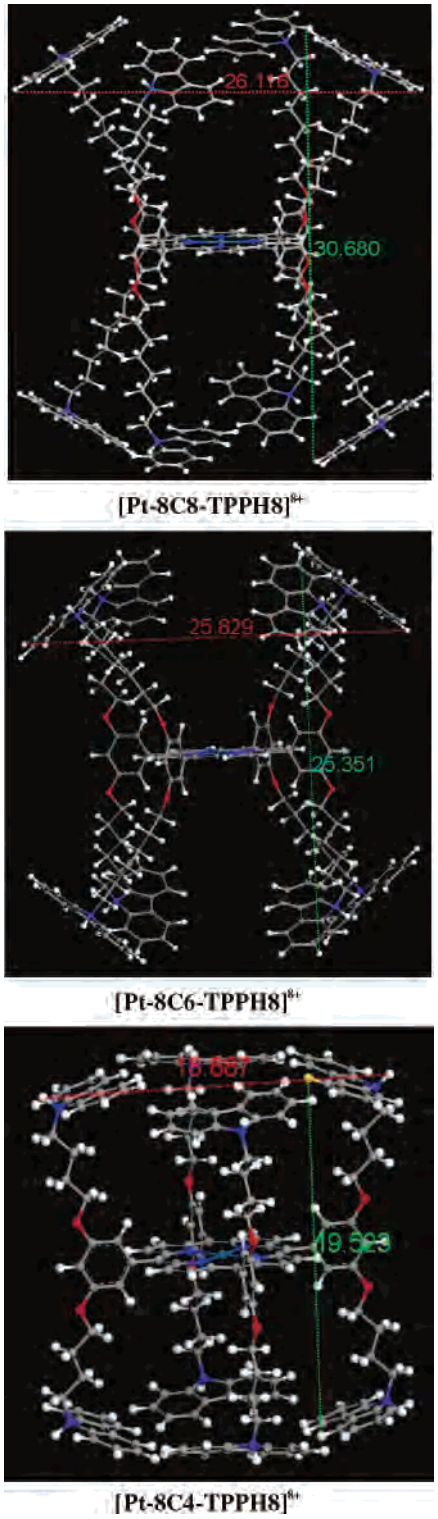

Figure 8. Molecular modeling structures of $[Pt\text{-}8C8\text{-}TPPH8]^{8+}$, $[Pt\text{-}8C6\text{-}TPPH8]^{8+}$, and $[Pt\text{-}8C4\text{-}TPPH8]^{8+}$.

MCM-48 is big enough for the dimensions of the $[Pt\text{-}8C4\text{-}TPPH8]^{8+}$ molecule. As a result, $[Pt\text{-}8C4\text{-}TPPH8]^{8+}$/MCM-48 displays a common oxygen sensing property similar to that of $[PtTMPyP]^{4+}$/MCM-41 ($[PtTMPyP]^{4+}$ = platinum *meso*-tetrakis(4-*N*-methylpyridyl)porphyrin) assembly materials that were reported by us recently.[29]

To further confirm above explanation, $[PtTMPyP]^{4+}$ molecules was employed as chromophores to assemble the oxygen sensor $[PtTMPyP]^{4+}$/MCM-48. The approximate dimensions of $[PtTMPyP]^{4+}$ are 1.9 nm × 1.9 nm × 0.5 nm, which are estimated from the modeling calculation results. Although $[PtTMPyP]^{4+}$ has only four side chains and a lower charge compared with $[Pt\text{-}8Cn\text{-}TPPH8]^{8+}$, it could be easily adsorbed into the pores of mesoporous silicas. The cation exchange[28,29,46,47] between the protons of silanol groups on the surface of MCM-48 and $[PtTMPyP]^{4+}$ plays a role in the adsorption process. On the other hand, the pore dimension of MCM-48 is larger than that of the $[PtTMPyP]^{4+}$ molecules. The luminescent spectral change of $[PtTMPyP]^{4+}$/MCM-48 (20 mg/g) is presented in Figure 9. The relative luminescent intensity of $[PtTMPyP]^{4+}$/MCM-48 (20 mg/g) decreases by 98.0% upon changing from pure nitrogen to pure oxygen. The Stern−Volmer plot (Figure 10) of $[PtTMPyP]^{4+}$/MCM-48 (20 mg/g) shows that the value of I_0/I_{100} is 49.6. The detailed oxygen sensing properties of $[PtTMPyP]^{4+}$/MCM-48 with different $[PtTMPyP]^{4+}$ loading levels are presented in Table 2. The oxygen sensing performance of $[PtTMPyP]^{4+}$/MCM-48 is better than that of $[Pt\text{-}8C4\text{-}TPPH8]^{8+}$/MCM-48. The pore dimension of MCM-48 is large enough for the $[PtTMPyP]^{4+}$ molecules. Even though some $[PtTMPyP]^{4+}$ molecules are encapsulated in the pores of MCM-48, there is still excess space to allow oxygen molecules to transport freely, so oxygen molecules can easily diffuse into/out of the pores of $[PtTMPyP]^{4+}$/MCM-48. The molecular dimensions of $[Pt\text{-}8C4\text{-}TPPH8]^{8+}$ are bigger than those of $[PtTMPyP]^{4+}$. As some $[Pt\text{-}8C4\text{-}TPPH8]^{8+}$ molecules are adsorbed, the pores of MCM-48

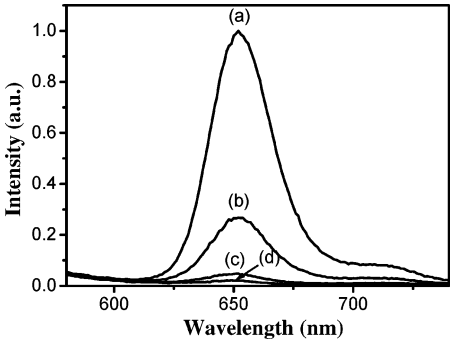

Figure 9. Emission spectra of $[PtTMPyP]^{4+}$/MCM-48 (20 mg/g) under different oxygen concentrations: (a) 0; (b) 1; (c) 10, and (d) 100% oxygen.

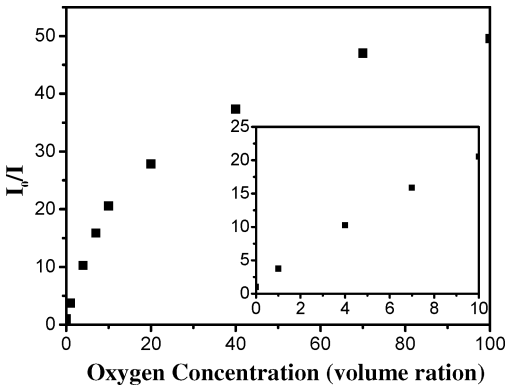

Figure 10. Stern−Volmer plot for $[PtTMPyP]^{4+}$/MCM-48 (20 mg/g) at different concentrations of oxygen. Inset: Stern−Volmer plot at low oxygen concentration.

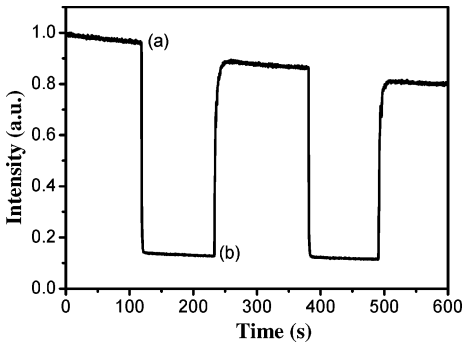

Figure 11. Response time and relative intensity change and reproducibility for [Pt-8C4-TPPH8]$^{8+}$/MCM-48 (20 mg/g) on switching between 100% nitrogen (a) and 100% oxygen (b).

are partially blocked and the oxygen molecules cannot pass freely through the pores. Therefore, [PtTMPyP]$^{4+}$/MCM-48 exhibited better oxygen sensing performance than [Pt-8C4-TPPH8]$^{8+}$/MCM-48. Figure 11 shows the response property of [Pt-8C4-TPPH8]$^{8+}$/MCM-48 (20 mg/g). Upon increasing oxygen concentration, the emission intensity drops quickly, while upon decreasing oxygen concentration, the emission intensity cannot recover to the initial level under 100% nitrogen again. When the sample is exposed to an alternating atmosphere of nitrogen and oxygen, it is observed that the emission intensity decreases gradually. A possible explanation for this phenomenon is that some oxygen molecules were confined inside in the pores of MCM-48 by [Pt-8C4-TPPH8]$^{8+}$ molecules, resulting in the emission quenching of [Pt-8C4-TPPH8]$^{8+}$. It was found that the emission intensity could recover to the initial level under nitrogen if the sample was treated for 2 h under a vacuum condition. For [PtTMPyP]$^{4+}$/MCM-48, a similar phenomenon also was observed, but the decreasing tendency of the emission intensity is not marked compared with [Pt-8C4-TPPH8]$^{8+}$/MCM-48 (see Supporting Information, Figure S34).

The values of I_0/I_{100} for [Pt-8C4-TPPH8]$^{8+}$/MCM-48 with different loading levels are 5.3 (10 mg/g), 5.7 (20 mg/g), and 4.1 (40 mg/g), respectively. [Pt-8C4-TPPH8]$^{8+}$/MCM-48 displays a luminescence-quenching maximum at the loading level of 20 mg/g, and the I_0/I_{100} value of [Pt-8C4-TPPH8]$^{8+}$/MCM-48 (10 mg/g) is near that of [Pt-8C4-TPPH8]$^{8+}$/MCM-48 (20 mg/g) while [Pt-8C4-TPPH8]$^{8+}$/MCM-48 (40 mg/g) exhibits an obviously minor I_0/I_{100} value compared with that of [Pt-8C4-TPPH8]$^{8+}$/MCM-48 (10 mg/g or 20 mg/g). For the [Pt-8C4-TPPH8]$^{8+}$/MCM-48 (40 mg/g) sample with higher loading level, a few [Pt-8C4-TPPH8]$^{8+}$ molecules may be adsorbed into the deeper positions of the pores of MCM-48 and are encapsulated inside by some other [Pt-8C4-TPPH8]$^{8+}$ molecules that lie at the shallower position of the pores. Under this situation, oxygen molecules cannot quench the luminescence of the [Pt-8C4-TPPH8]$^{8+}$ molecules that are located at the deeper positions of pores because oxygen molecules could not reach their locations. Therefore, [Pt-8C4-TPPH8]$^{8+}$/MCM-48 (10 mg/g and 20 mg/g) displays a more efficient luminescence quenching property than [Pt-8C4-TPPH8]$^{8+}$/MCM-48 (40 mg/g).

Conclusions

In conclusion, a series of luminescent platinum porphyrins Pt-8C*n*-TPP with eight alkyl−carbazole arms were synthesized. The protonated porphyrins [Pt-8C*n*-TPPH8]$^{8+}$ were employed to assemble with mesoporous silica MCM-48. Assembly materials [Pt-8C*n*-TPPH8]$^{8+}$/MCM-48 were used as optical oxygen sensors. We demonstrated that [Pt-8C8-TPPH8]$^{8+}$/MCM-48 and [Pt-8C6-TPPH8]$^{8+}$/MCM-48 are oxygen sensing materials with a high sensitivity and fast response time. The assembly materials possess very high sensitivity, linear Stern−Volmer characteristics at low oxygen concentration, and very fast response properties, which are beneficial to the applications.

Acknowledgment. This work was supported by the National Natural Science Foundation of China (50225313, 50520130316, and 50573030), the Major State Basic Research Development Program (2002CB613401), the Program for Changjiang Scholars and Innovative Research Team in University (IRT0422), and the Program of Introducing Talent of Discipline to Universities (B06009).

Supporting Information Available: The absorption and emission spectra of Pt-8C6-TPP and Pt-8C6-TPP in solution and solid states and the detailed oxygen sensing properties of all other assembly materials. These materials are available free of charge via the Internet at http://pubs.acs.org.

IC060354C